

See discussions, stats, and author profiles for this publication at: <https://www.researchgate.net/publication/51182379>

# Svatoš A.. Single-cell metabolomics comes of age: new developments in mass spectrometry profiling and imaging. Anal Chem 83: 5037-5044

ARTICLE *in* ANALYTICAL CHEMISTRY · JUNE 2011

Impact Factor: 5.64 · DOI: 10.1021/ac2003592 · Source: PubMed

---

CITATIONS

50

---

READS

21

## 1 AUTHOR:



**Ales Svatos**

Max Planck Institute for Chemical Ecology

**258** PUBLICATIONS **5,424** CITATIONS

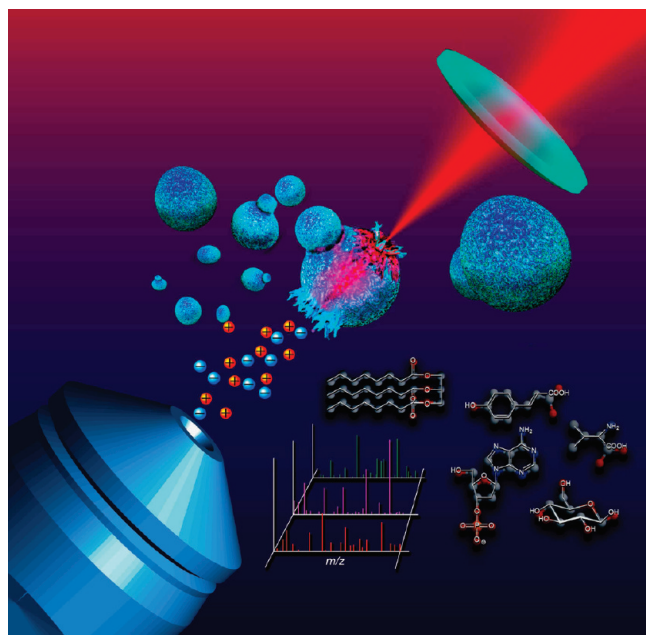
SEE PROFILE

# Single-cell metabolomics comes of age: new developments in mass spectrometry profiling and imaging

Modern mass spectrometry is ready to explore individual cell metabolomes, and 4 massive advances in medicinal and biological applications may be expected in a near future.

Aleš Svatoš

Max Planck Institute for Chemical Ecology (Germany)



Robert Gates

Progress in biology and related areas of the biosciences depends on technological advances. The ability to visualize biological materials or tissue samples has long helped scientists to map the distribution of organs, organelles, and cells and thus better understand the principles of life. Most methods to date have relied on microscopy and different staining techniques. These methods have led to many important discoveries but lack molecular specificity. To analyze a metabolite directly, scientists have recently developed alternative methods to visualize or image tissues or cells; these include observing the compound-specific vibration or resonance with spectroscopy techniques such as UV–vis, IR,<sup>1</sup> coherent anti-Stokes Raman spectroscopy (CARS),<sup>2</sup> or NMR<sup>3</sup> or directly measuring a compound's mass with MS (Figure 1). Together with the labeling approaches, these direct methods add new dimensions to our ability to analyze single cells.

The term “single cell” has different connotations for different scientific disciplines. Some macroalgae are single celled and several centimeters wide; some bacterial cells are as small as 1  $\mu\text{m}$ . Current MS techniques<sup>4</sup> are capable of imaging a sample object as small as 2–3  $\mu\text{m}$ , and scientists are close to being able to “see” the inner chemical composition of bacterial cells. Although

numerous reviews have recently been published<sup>5–11</sup> on this topic, a comprehensive and critical overview of the most current advances (2008–2011) is of general interest.

During the last 15 years, technology in the “-omics” sciences has made substantial progress, especially in the areas of genomics and transcriptomics, allowing single-cell transcriptomic studies.<sup>7</sup> Accordingly, metabolomics, the determination of a set of small molecules known as metabolites (<2500 Da with a typical molecular weight of 400 Da) in organisms or cells, has flourished.<sup>12</sup> However, metabolomics is still waiting for the discovery of a method that puts it on par with genomics in terms of throughput and sensitivity. In contrast to genes and proteins, metabolites have much greater structural diversity: they are not simply combinations of 4–20 letters of the gene or protein alphabet. Furthermore, they must be determined at native concentrations because no general amplification protocol for metabolites exists. Yet despite these problems, the information metabolites offer is essential for understanding life because they are responsible for organisms' phenotypes.

The two principal methods in metabolomics that are used to detect and structurally elucidate metabolites are NMR and MS. The latter possesses much higher sensitivity and selectivity and can be easily combined with other diverse separation methods such as GC or LC, and most metabolic studies are performed on these hybrid instruments. These provide information about the mass of detected ions and fragmentation spectra, and the molecular formula of a metabolite can be determined from the accurate mass. The fragmentation spectra, which provide information about the presence of functional groups in and the molecular structure of compounds, can be compared to in-house builds or commercial databases, matched to the spectra of standards, or correlated to compound classes using computational approaches.<sup>13</sup> GC/MS is useful for volatile, thermally stable metabolites or for primary metabolites (sugars, amino acids, etc.) only after appropriate derivatization (hydroxylation and silylation).<sup>14</sup> LC/MS is used for a much more diverse and interesting compound class, so-called secondary metabolites that have limited thermal stability. Mild ambient ionization methods such as ESI, atmospheric pressure chemical ionization, or atmospheric pressure photoionization are used after the compounds of interest are separated by LC or CE systems. In addition, MALDI is a direct profiling and imaging method for metabolites up to the size of large biomolecules.

Published: June 01, 2011

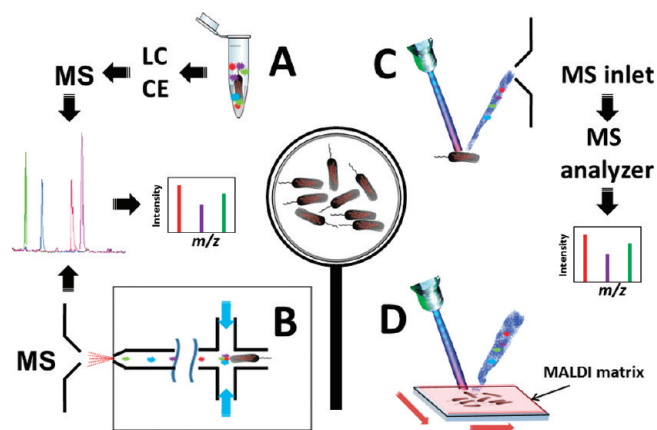


**Figure 1.** Schematic representation of current methods of single-cell MS-based profiling and imaging.

Signals in  $^1\text{H}$ -NMR spectra using high-field magnets are relatively well dispersed across the spectral width, and their integrals correspond to the number of hydrogen atoms attached to the functional group/molecule. Association of the  $^1\text{H}$ -NMR signals with individual metabolites allows exact quantification of the metabolites.<sup>15</sup> However, obtaining the signal correspondence matrix typically requires acquiring 2D NMR correlation spectra, and in small sample amounts, the limit of detection often becomes too high to be useful. With some compromises, NMR can be combined with LC separation, and if both are used, the sensitivity for 1D  $^1\text{H}$ -NMR spectra will be in the range of picomoles. Other spectroscopic methods, such as IR, Raman, UV–vis, and fluorescence spectroscopy, provide some degree of structural specificity and can be very useful for identifying unique structural types of metabolites; however, these lack the general applicability of MS and NMR methods.

## TECHNICAL ASPECTS

Typically, metabolomics<sup>16</sup> starts with harvesting the studied object; depending on the aim of the investigation, some parts (such as leaves of plants) may be detached. The samples are homogenized, after which inhibitors preventing oxidation and enzymatic degradation may be added. The metabolome is extracted from cells with particular solvents, and the tissue debris is removed by centrifugation or filtration. Samples can be analyzed directly or partially separated according to their mass or polarity or, if MS is used, can be derivatized to become compatible with the ionization method. To obtain quantitative data, samples must be spiked with standards (preferentially labeled with stable isotopes) in the early stages of sample preparation. When sampling at cellular and subcellular levels, this protocol becomes impractical because the amount of contamination originating from solvents and the extraction apparatus may dramatically increase, and the signals of interest may be lost in the contaminant-related noise.

The earliest studies of single cells were performed without sample preparation using the MALDI TOFMS method.<sup>17</sup> Cells were deposited on the metallic target and treated with MALDI matrix solutions. The matrix and solvents extracted metabolites/peptides from the cells, and the matrix assisted their desorption/ionization. Interestingly, peptides from neural cells were first analyzed concurrent with the development of the MALDI MS imaging (MSI) method.<sup>18</sup> MALDI is still a very attractive method

and can perform cellular analysis in an imaging mode that allows different areas to be selectively irradiated with the laser foci bigger than the cell dimension using oversampling protocol.

## COMPETING TECHNOLOGIES

Hell and others have developed innovative microscopic methods that allow fluorescently labeled proteins to be observed at a 10 nm resolution. Hell and coworkers broke the Abbe diffraction limit by developing stimulated emission depletion (STED) fluorescence microscopy<sup>19</sup> and have discovered the nonlinear de-excitation of fluorescent dyes. STED was recently combined with scanning electron microscopy to provide topological information on cells that can be combined with the spatial localization of individual proteins. IR and Raman microscopy methods have been improved by implementing CARS and, more recently, stimulated Raman scattering (SRS) systems.<sup>20</sup> In contrast to CARS, SRS provides the correct Raman vibration frequencies; as a result, the visualized chemical species can be easily identified or characterized using existing Raman spectra atlases. Despite this dramatic improvement, spectroscopy methods are limited in their ability to characterize the structure of individual metabolites. Current improvements in NMR sensitivity notwithstanding, imaging and metabolomic studies on the cellular level are possible only after special preparation techniques such as laser microdissection.<sup>21</sup> High-resolution imaging studies are limited to mapping differences in relaxation times or proton spin density (magnetic resonance microscopy) and the chemical shift imaging of high-abundance compounds (e.g., assimilated sugars in plant vascular bundles).<sup>22</sup> However, the fundamental methodology for MRI at micrometer resolution is under development.<sup>23</sup>

Unlike the methods described so far, MS destroys analyte molecules; however, it has the potential to precisely characterize and identify metabolites with high sensitivity. The spatial resolution achieved by one of the initial methods for MS imaging, secondary ion MS (SIMS), is comparable to that achieved by STED or CARS; however, the high-energy particles needed to evaporate and ionize chemical compounds from the target are destructive to most metabolites, and SIMS can detect only compound-class-specific ions at 10 nm resolution. Nano-SIMS can be used to study biological phenomena such as changes in the calcium dynamics in cells, microelement allocation in cell compartments,<sup>24</sup> or metabolic exchanges using stable isotopic labeling in bacterial communities or biofilms.<sup>25</sup> Milder ionization methods such as ESI or MALDI have not yet been able to study phenomena  $<1\ \mu\text{m}$ , but many laboratories are hard at work on this challenge.

## INNOVATIVE SAMPLE PREPARATION AND CELL MANIPULATION

Sample preparation, the most critical step in metabolomics, is still problematic in the cellular range. If the object is cellular, such as bacteria, yeast or fungi, microfluidics seems to be the most appropriate way to sort, concentrate, disintegrate, and extract cells.<sup>5,6,26,27</sup> In multicellular organisms, individual cells can be separated from each other by cellular matrix lysis before the microfluidic step, but it is important to show that such manipulation does not alter the metabolomic and developmental state of the studied cells. Probably the best way of preventing stress is to keep the sample under ambient conditions. Combining sample preparation directly with the gasification and ionization

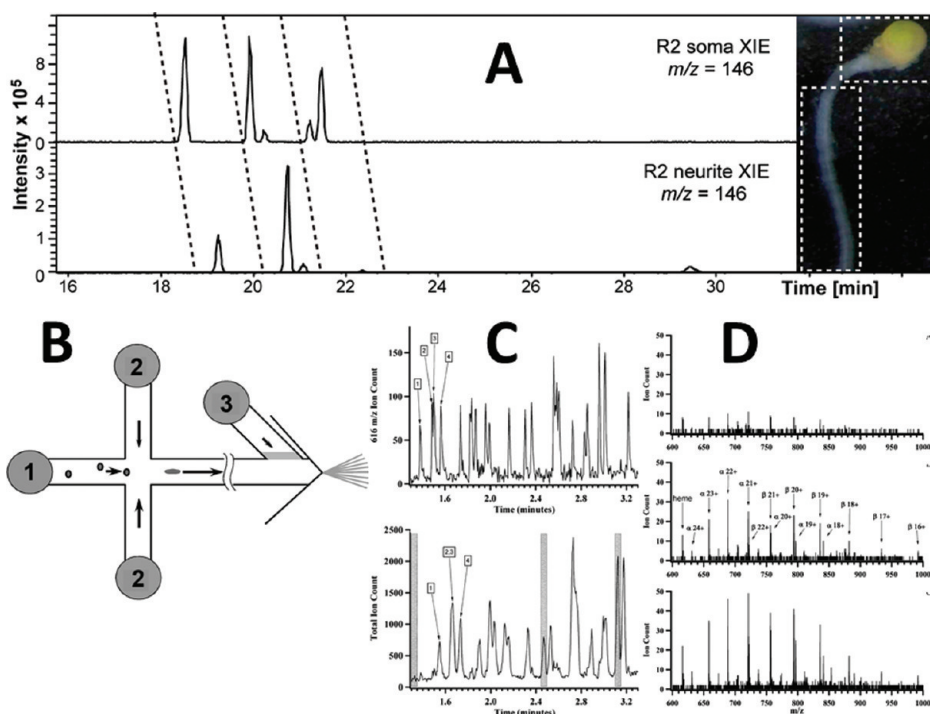


**Figure 2.** CE/MS-based single-cell metabolomics. A) A section of electropherogram obtained for an extract of dissected *A. californica* R2 neuron soma (top) and neurite (bottom) showing distinct single-ion profiles plotted for  $m/z$  146 representing acetylcholine (the far left peak) and unidentified isobaric compounds. B) Schematic diagram showing the basic operation of the cell lysis CE/MS microchip. Reservoirs are labeled 1 (cells), 2 (buffer), 3 (side channel); the separation channel is 4.7 cm long. C) Ion count at  $m/z$  616, corresponding to the hemoglobin-released protonated heme (top) and the background subtracted total ion count (bottom) for a 2 min segment of the continuous lysis plus CE/MS experiment. Individual cell lysis events are marked 1–4. D) Mass spectra generated by summing the data in each of the 3 s windows illustrated by gray rectangles in (C). The top trace corresponds to the baseline, the middle trace corresponds to a single cell lysis event, and the bottom trace corresponds to the lysis of multiple cells. Both the  $\alpha$ -form and the  $\beta$ -form of hemoglobin are visible. Reproduced from refs.38 (A) and 27 (B–D).

of metabolites is the gentlest preparation method and has been recently used in cell-addressable laser-assisted ESI (LAESI) at  $\sim 30 \mu\text{m}$  resolution.<sup>28</sup> Because finding the proper position is problematic if micrometer scales are used, a blind method using MSI technology<sup>29</sup> in which metabolites are desorbed and ionized from a predefined x,y-grid can simplify this issue.

## MS TECHNOLOGIES AND METHODS FOR SINGLE-CELL IMAGING AND METABOLOMICS

**Innovative sample preparation combined with separation methods and MS detection.** Increasing spatial resolution is associated with the obvious problem of decreasing amounts of molecules detectable from the sample. The UV laser, which is able to penetrate a maximum of  $200 \text{ nm}^3$  into the sample and at spot size  $1 \mu\text{m}$ , can theoretically sample  $6 \times 10^9$  water molecules, or  $\sim 6 \text{ nmol}$ . Typical concentrations of abundant metabolites in cells are in the millimolar to micromolar range, and the ionization process and subsequent measurements have  $\sim 0.001$ – $0.1\%$  efficiency;<sup>30</sup> therefore, performing cellular metabolomic measurements for major metabolites requires low femtomolar to high attomolar sensitivity. Nevertheless, the sensitivity of current MS instrumentation is not sufficient to trace much less abundant yet important signal molecules operating intra- and intercellularly.

The simplest way to analyze cell content is to capture cells by microsampling under a microscope using micromanipulators holding sharp tools.<sup>31</sup> Although single glands from a pitcher of carnivorous plants of the genus *Nepenthes* were dissected and

mRNA successfully extracted and amplified, no metabolite analysis was performed.<sup>31</sup> Laser-assisted micro-dissection techniques can separate larger cells and cell populations from tissue, and conventional MS (Figure 1A) and cryogenic NMR methods can analyze the cell(s).<sup>21</sup> However, cell content is often contaminated by membranes and debris from neighboring cells.

Scientists in Japan obtained cleaner samples by combining video-microscopy with nano-ESI microcapillary tubes handled by a micromanipulator to pierce cells<sup>32–35</sup> and draw  $\sim 1$ – $5 \text{ pL}$  of their internal contents into the capillary tube. The thick liquid is diluted with water or organic solvent containing a volatile acid or base and introduced into a nano-ESI source holder. Rich MS spectra can be recorded, and up to 1000 mass features detected in  $\sim 5$ – $10 \text{ min}$ . The longer spraying time allows for numerous collision induced dissociation (CID) experiments to be performed and metabolites to be rigorously identified. This method identified serotonin and histamine from mast cells and determined their localization in cellular space.<sup>35</sup> Clearly, this method has great potential for detailed cell analysis and “error-free” sampling.

In addition to this method, abbreviated live single-cell MS (LiveSC/MS) has been used to study plant cells with similarly encouraging results.<sup>34</sup> Recently, another group modified LiveSC/MS by using the etched hollow-fiber sampling tip as a UV-laser light guide.<sup>36</sup> The focused laser beam lyses the individual cells, and the cell content is guided into the capillary tube under video surveillance. After the sample is transferred into PCR vials and diluted with  $0.1\%$  formic acid ( $10 \mu\text{L}$ ), the entire



volume is injected on a trapping column and analyzed by LC/ESI MS/MS. Analysis of individual mesophyll oat (*Avena sativa* L.) cells showed a temporal and spatial pattern of avenanthramides phytoalexins that had accumulated as a result of stress or treatment with elicitors.<sup>36</sup> The typical volume of cell content was 10–40 pL, and avenanthramides were identified by comparing CID spectra with those of authentic standards.

Stable isotope labeled congeners and multiple reaction monitoring transitions were used to quantify the amount of phytoalexins. Extensive accumulation of phytoalexins A and B was observed 12 h (1 and 400 amol per cell, respectively) after elicitor treatment with a maximum at 24 h (2.5 and 900 amol per cell, respectively). Similarly, single pavement, basal, or trichome cells from *Arabidopsis thaliana* leaf surface were pierced by a pool-out glass capillary (aperture 1–10  $\mu\text{m}$ ) held in a micromanipulator, and primary metabolites identified and quantified on a GC/MS.<sup>37</sup>

LiveSC/MS has great potential for detailed qualitative and quantitative studies of cellular metabolomes for which high throughput and automation are not required. However, an elaborate experimental setup or the need for expensive micromanipulators or confocal microscopy hardware could prevent its widespread use. What is encouraging is that the very rich MS spectra obtained from individual cells show that the individual metabolome is within reach of current MS methods if ESI is used for ionization.

Members of the Sweedler lab<sup>38</sup> have used CE coupled to a Q-TOF mass spectrometer to separate and detect neurotransmitters in a complex mixture extracted from dissected *Aplysia californica* neural cells. The very high separation efficiency of the CE instrument (600,000 theoretical plates  $\text{m}^{-1}$ ) and innovative sheath-flow interfacing of the CE instrument to the MS nano-ESI source (250  $\text{nL min}^{-1}$ ) provided very high sensitivity in the attomolar range for acetylcholine, serotonin, dopamine, and histamine. The 6 nL that was hydrodynamically injected on the CE capillary inlet corresponds to a concentration of  $\sim 50$  nM analyte. Single-cell analysis was demonstrated on dissected *A. californica* R2 cholinergic neurons. After being desalted, the cell was extracted with an acidified aqueous methanol solution (5  $\mu\text{L}$ ), and 0.1% of the extract was analyzed on the CE/ESI MS setup. Approximately 100 metabolites were detected at <25 ppm mass accuracy with  $10^4$  ion count intensities, and those intense precursors afforded strong CID spectra that could be used to identify the metabolites. Different metabolites were detected in neurite and soma (Figure 2A).

Combining the CE/MS with the sample preparation used in the LiveSC/MS might provide the long-sought solution for single-cell metabolomics. However, a suitable device for cell sampling, disintegration, and extraction still needs to be developed, possibly using a microfluidic platform or laser tweezers combined with extraction nanovials. A microfluidic electro-osmotically pumped electrophoretic chip coupled to ESI MS (Figure 1B and 2B) was recently shown to be an excellent solution for individual cells.<sup>27</sup> Human erythrocytes suspended in a low ionic strength buffer flowing from reservoir C (Figure 2B) were individually lysed by rapidly increasing the ionic strength of a strong buffer flowing from reservoir B, after which the cell content was separated in an electrophoretic chip channel; ultimately, the released molecules were detected in the mass spectrometer. Lysis events in individual cells correspond to peaks in the resulting total ion current (Figure 2C), and plots of individual ions, such as those at  $m/z$  616 for protonated heme or signals for hemoglobin  $\alpha$ - or  $\beta$ -chains (Figure 2D), show the separation of small metabolites and larger proteins.

This groundbreaking work shows that the internal content of a very small cell (6–8  $\mu\text{m}$ ) could be individually assayed and that the simultaneous determination of metabolites and proteins is possible. If the sensitivity of the method is increased, it could also open a new area in clinical applications in which a limited amount of sample is available.

## METHODS WITH FOCUSED BEAMS OF IONS OR LIGHT

**Cluster SIMS.** The primary direct method (without a separation step) for studying cell metabolites is SIMS. Organic SIMS was introduced by Benninghoven in 1978 and later extended by Winograd.<sup>39</sup> Here, a tightly focused primary beam of high-energy charged particles or ions eject and ionize molecules (secondary ions) of interest from the sample. Recently, by using  $\text{C}_{60}^{+\bullet}$ ,  $\text{SF}_5^+$ , and ionic cluster ( $\text{Au}_n^+$ ,  $\text{Bi}_n^+$ ,  $\text{SF}_5^+$ ) primary beams and treating samples with matrix or nanoparticles, small stable molecules within a cell have been imaged with excellent spatial resolution, allowing 3D maps of their distribution to be constructed.<sup>40</sup> In addition, cluster SIMS using a  $\text{C}_{60}^{+\bullet}$  ion gun has been interfaced to hybrid Q-TOF instrumentation, providing excellent mass resolution and accuracy and enhancing the identification power of SIMS imaging. The secondary ions that are formed are collisionally cooled by nitrogen gas, and the instrument's performance is comparable to that used in TOF SIMS.<sup>41</sup> Solving the technical problems of positioning a  $\text{C}_{60}^{+\bullet}$  ion source into hybrid MS instruments<sup>42</sup> has opened the way for high spatial resolution imaging and cell profiling; proteomic and metabolomic laboratories around the world will hopefully soon use SIMS technology to solve biological questions.

**UV-MALDI and LDI ionization.** Using the laser desorption/ionization (LDI) or MALDI methods with tightly focused laser beams, scientists can achieve high sampling efficiency and spatial resolution. LDI does not use matrices, which eliminates sample preparation (Figure 1C). The commercial SmartBeam laser in Ultraflex II and III mass spectrometers allowed cellular features on *Arabidopsis thaliana* petals and sepals and storage cavities in *St. John's Wort* (*Hypericum perforatum*) as small as 10  $\mu\text{m}$  to be observed.<sup>43</sup> A scanning microprobe matrix-assisted laser desorption/ionization (SMALDI) source achieved even better spatial resolution. SMALDI combines a custom-built atmospheric pressure source for focusing lasers to a few microns with a commercial Orbitrap XL (Thermo) instrument. The latter is used to provide high lateral and mass resolution and accuracy and molecular histology on a cellular scale.<sup>44</sup> In addition to the high mass resolution it provides, this method allows MS/MS experiments to be performed.

The power of the SMALDI atmospheric probe has been well documented for MSI of a thin section of a mouse pituitary gland at 5  $\mu\text{m}$  spatial resolution<sup>45</sup> (Figure 3A). Even a single-pixel FTMS spectrum from the posterior (Figure 3B) or the intermediate lobe (Figure 3C) shows very rich MS spectra acquired at high mass resolution and accuracy, providing tentative assignment for diacetyl- $\alpha$ -melanocyte-stimulating hormone, oxytocin, and vasopressin peptides with at least 1.5 ppm mass accuracy (Figure 3B and C). The areas secreting/accumulating those three peptides are very tightly localized to the expected mouse pituitary gland subsections (Figure 3D and E). Further confirmation of peptide identity was performed via database searching with a slightly modified spatial resolution (10  $\mu\text{m}$ ), which allowed enough precursor ions to be submitted to CID experiments.

SMALDI scanning still requires a matrix, and the spatial resolution can be influenced by crystal size. A two-step protocol

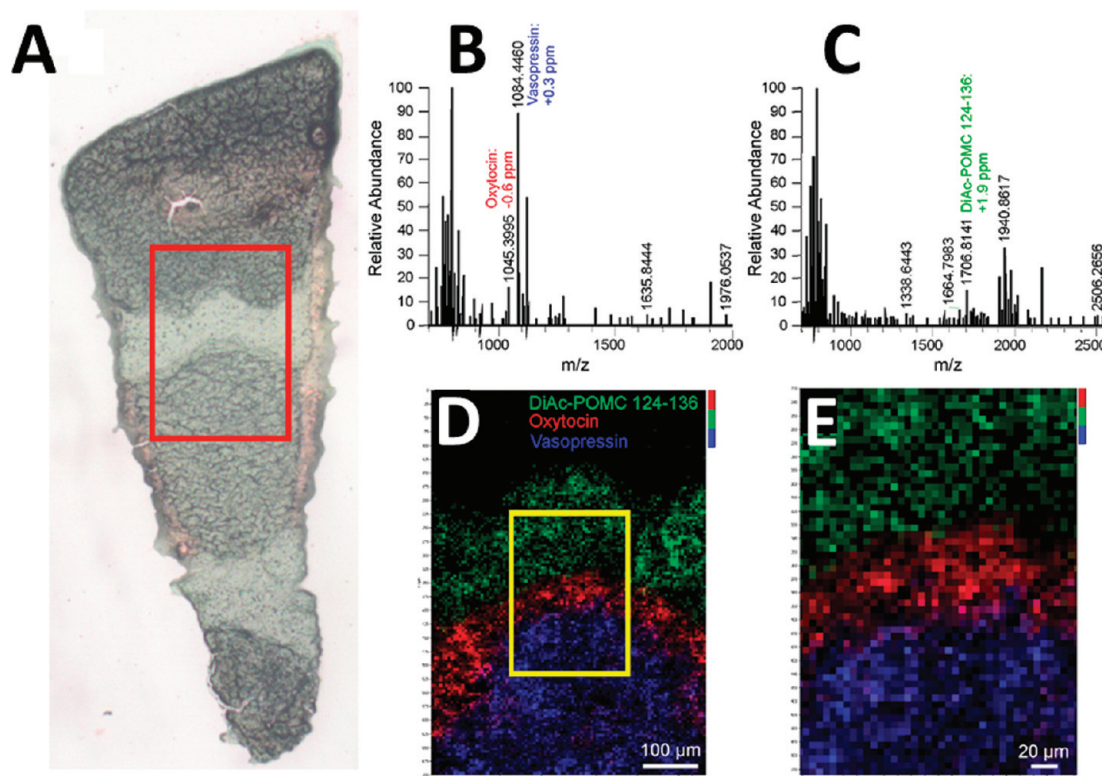


**Figure 3.** MSI on Orbitrap XL instrument with SMALDI probe fitted at  $5\ \mu\text{m}$  spatial resolution. A) Micrograph of a thin section of mouse pituitary tissue with the region imaged indicated by a red square. B) Single-pixel FTMS spectrum from the posterior lobe and C) from the intermediate lobe. D) Overlay of ion images for diacetyl- $\alpha$ -MSH (DiAc-POMC 124–136; green), oxytocin (red) and vasopressin (blue); pixel size  $5\ \mu\text{m}$ . E) Enlarged view of the border between intermediate and posterior lobe documenting  $5\ \mu\text{m}$  spatial resolution. Reproduced with permission from ref. 45.

was developed for the application of matrix for SMALDI: matrix sublimation followed by matrix recrystallization in water vapor.<sup>46</sup> Very fine crystals were obtained, allowing a  $2\ \mu\text{m}$  lateral resolution of the neuropeptide substance P to be achieved. This technology will soon be available commercially. Although further improvement in lateral resolution is limited by the low number of ions formed from the small irradiated area, future enhancements in the mass detection hardware or in improved MALDI matrices are expected to lower the spatial resolution to submicron spot sizes.

Tight laser focusing is not required to analyze yeast or algae cells if proper matrix and UV-laser oversampling are used (Figure 1D). Zenobi and colleagues<sup>4,47–51</sup> have developed methods that rely on 9-aminoacridine (9AA) negative mode MALDI TOFMS experiments and exhibit low attomolar to high zeptomolar sensitivity for phosphorylated central metabolites such as ADP, ATP, GTP, and UDP-glucose. Alternatively, a negative ion mode nanostructure-initiator mass spectrometer using 3-aminopropyldimethylethoxysilane was tested for some analytes; however, the sensitivity of the method was only in the femtomolar range.<sup>52</sup> The single-cell metabolomic analysis was demonstrated using large unicellular eukaryotic algae. A  $\sim 300\ \text{nL}$  aliquot of the cell suspension *Closterium acerosum*<sup>4</sup> (typically  $250\text{--}790\ \mu\text{m}$  long and  $25\ \mu\text{m}$  wide), which can grow in a diluted medium, was pipetted onto a stainless steel MALDI target. A high-resolution microscope with a digital camera was used to document and count cells. The droplets containing cells were treated with acetonitrile spiked with uridine 5'-monophosphate and an acetone solution of 9AA matrix. The principal component analysis revealed that the metabolite profiles of cells cultivated at cold temperatures ( $4\ ^\circ\text{C}$ ) were different

from the profiles of cells cultivated at warm temperatures ( $25\ ^\circ\text{C}$ ), and cells from each population could be distinguished in mixed populations. Human HeLa cells were mounted on indium tin oxide glass and after 6 h incubation in phosphate/saline buffer, were imaged using 9AA.<sup>53</sup> Rich negative mode MALDI MS spectra showing  $\sim 150$  individual signals were collected, and ATP, fructose-1,6-bisphosphate, and citrate were successfully identified, indicating single-cell metabolomic analysis is possible using MALDI MSI.

Followup work<sup>54</sup> indicated that metabolites of much smaller cells can be analyzed and that MALDI matrix selection is not limited to 9AA. Unicellular protist *Euglena gracilis* suspension was prepared as described previously, and 2,5-dihydroxybenzoic acid was used as the MALDI matrix. The preparation was scanned in an imaging mode using an x,y grid ( $2 \times 2\ \text{mm}$ ) with  $36\ \mu\text{m}$  pitch close to average cell size ( $50 \times 15\ \mu\text{m}$ ). Negative ion mode images were constructed from a rich MS spectra dataset in which diverse phospholipids were detected. The high-intensity ion counts were correlated with the positions of cells present. Some spots were well defined but some consisted of more than one pixel.

Recently, high-density microarrays were prepared by a laser ablation of an “omniphobic” layer (Figure 4A) deposited on a conductive support.<sup>51</sup> Cell suspension was applied, leaving none to several cells in each hydrophilic centers; the readout of phosphorylated metabolites (see above) was dependent on the number of cells (Figure 4B). The method is sensitive enough to allow the metabolites of individual yeast cells (*Saccharomyces cerevisiae*) to be measured and quantified. This work, which represents a major advance in MALDI-assisted cell analysis, offers a tool for unbiased metabolic profiling. Researchers in Sweedler’s laboratory use a



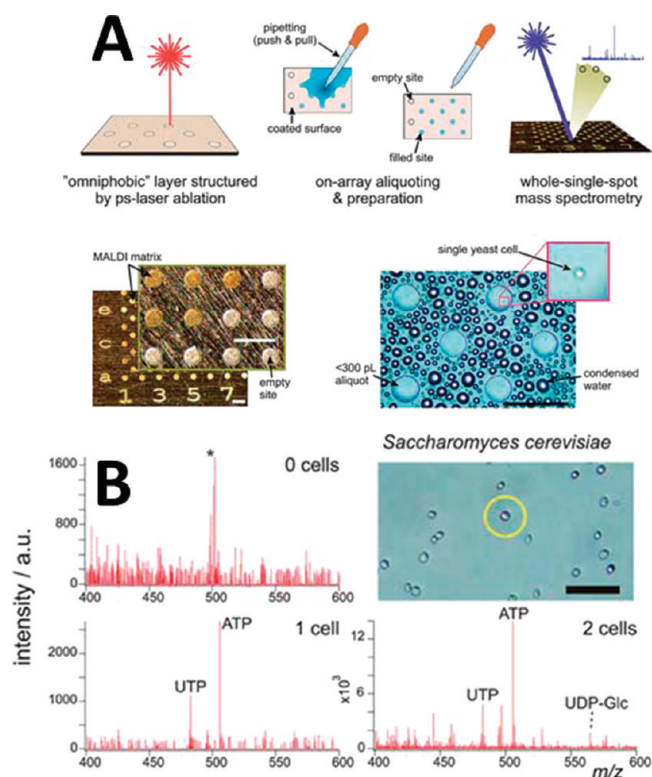


**Figure 4.** Microarrays for MS (MAMS). A) General workflow for the fabrication and application of MAMS. B) MALDI MS spectra of metabolites from 1–2 cells of *Saccharomyces cerevisiae*. Signal intensities correlate with number of cells present in the laser focal point. The signal marked with an asterisk (\*) corresponds to the matrix background. Scale bars: 50  $\mu\text{m}$ .

similar stretchable hydrophobic Parafilm support covered with micrometer-sized glass pearls to limit metabolite delocalization and focus the MALDI matrix on the measured cells.<sup>55</sup> This method has found application in neural cell metabolomics and peptidomics, but so far not elsewhere.

**IR-MALDI, LAESI.** The third method that can assay metabolites directly without sample preparation was developed when scientists in Vertes's lab combined an IR laser ( $\lambda \sim 2900 \text{ nm}$ ) with electrospray (LAESI, Figure 5A).<sup>28,56–58</sup> A germanium-oxide-based optical fiber tip was etched in diluted nitric acid,<sup>25</sup> providing a tip with the curvature radius of 15–50  $\mu\text{m}$ , which is held at a  $45^\circ$  angle  $\sim 30 \mu\text{m}$  above the sample surface during the IR laser pulses (Figure 5B). Intriguingly, when a cell was consecutively irradiated with several laser shots, a significant alteration of ion masses was observed. Such alteration was manifested in the different ratios of sucrose/fructose sodiated ions ( $m/z$  381 and 203, respectively) seen in *Allium cepa* epidermis cells. Shrestha and Vertes postulate that early laser shots (1st and 2nd) evaporated the extracellular volume and subsequent ones (3rd and 4th) evaporated cellular vacuoles, abundant organelles of plant cells.<sup>56</sup> Such analysis suggests the benefit of studying subcellular components, at least those of the bigger cells.

The next logical step was to adapt LAESI using a  $\text{GeO}_2$ -fiber-etched tip for imaging of *A. cepa* cells (Figure 5C and D).<sup>59</sup> In colorless cells, negligible concentrations of cyanidin accumulate (which are responsible for cells' coloration), but sucrose is typically present in both colorless and pigmented cells (with a preference for colorless). Sequentially opening neighboring cells proved that no mixing of the contents or degradation of the cellular metabolome occurs (Figure 5C and D). A similar experiment with a sour orange (*Citrus aurantium*) leaf containing a small ( $\sim 50 \mu\text{m}$ ) oil reservoir showed that when individual

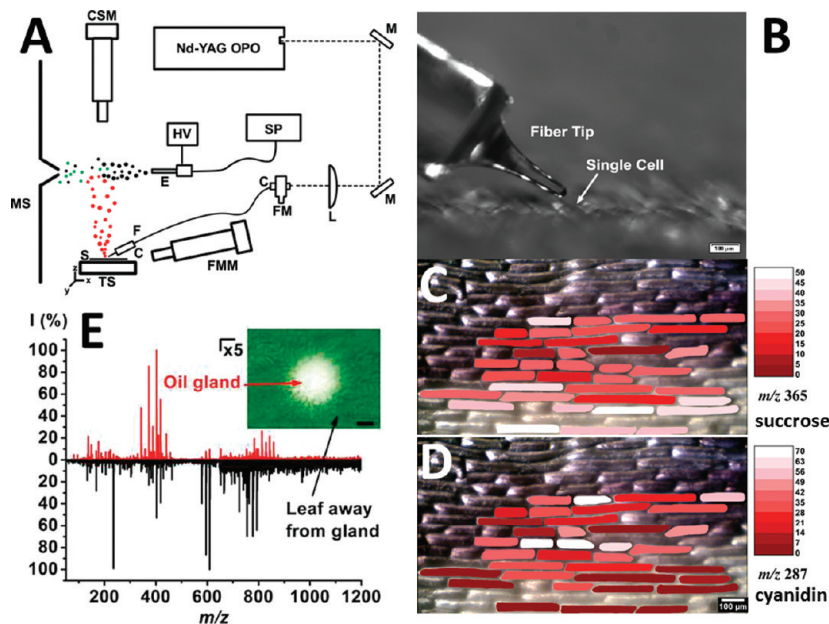


**Figure 5.** Cell-to-cell metabolic profiling and imaging using LAESI. A) Schematic of LAESI experimental setup. B) Etched  $\text{GeO}_2$  optical fiber tip  $30 \mu\text{m}$  above the surface of turgid epidermal cells from *A. cepa*. C) False color cell-by-cell chemical images of the metabolites cyanidin and D) sucrose were created by representing the ion intensities obtained from a cell on a color scale shown on right. MSI images show that cyanidin was selectively present in the number ( $n$ ) of pigmented cells ( $n = 20$ ), whereas it was virtually absent in the colorless cells ( $n = 16$ ), and sucrose was uniformly distributed throughout the entire studied cell population. (E) Positive-ion LAESI mass spectra from oil gland cells ( $n = 6$  to  $8$ ) of a *C. aurantium* leaf (red trace on top) and  $n = 6$  to  $8$  cells from the leaf away from the gland (black trace on bottom). The inset shows a micrograph of an oil gland before ablation. Scale bar:  $20 \mu\text{m}$ . Reproduced from refs. 28 (A) and 59 (B–D).

cells were analyzed, several terpenes could be identified in the oil reservoirs (Figure 5E).

Despite the exciting range of possibilities LAESI offers, it has some limitations: the ion intensities in images may be influenced by the water concentration in samples because the matrix is either water or compounds containing hydroxyl groups. So far, all single-cell experiments have been performed on flat surfaces with a GaO<sub>2</sub>-fiber-etched tip kept ~30 μm from the surface. Further technological development to automatically adjust the tip so it can be used for automatic cell-to-cell imaging and to adjust laser focus on samples with complicated topography such as trichome-rich plant leaves is needed.

## SUMMARY AND OUTLOOK

Two methods capable of viewing the metabolome at the cellular and subcellular levels are reported in detail above. In the first approach single cells or their contents are collected, and after dilution/extraction in a vial, metabolites (~100–1000 per cell) are chromatographically separated and analyzed with a mass spectrometer. These methods suffer from limited throughput, but this limitation was recently overcome by combining in-chip cell lysis with CE separation. In the second approach, cell content is assayed using ion beams or lasers and ions are quickly detected without separation. Sampling of larger areas can provide 2D or 3D metabolomic maps. Ion mobility separation can reduce sample complexity similar to chromatographic separation before ionization. Both approaches are complementary, and their combination is advised. Gradual improvements in current methods as well as novel concepts such as use of atomic force microscopy or scanning near-field optical microscope tips for the nonlinear enhancement of the laser<sup>60,61</sup> bring the promise that submicrometer resolution will be achieved without compromising on further ion analysis.

Breakthrough technologies such as SMALDI and LAESI are close to being commercially available, and biologists could soon start to harvest the tremendous potential of these methods. For example, using qualitative and quantitative metabolomics to determine the phenotype of individual cells in dissected or cryo-sectioned organs should be feasible in the near future, allowing primary and secondary metabolites, as well as peptides or proteins, to be localized and their concentrations to be assayed. Because some of featured novel interfaces can be attached to existing mass spectrometers fitted with atmospheric ionization sources, in vivo studies will be highly cost effective.

As mentioned, individual techniques for sample preparation and orthogonal imaging methods must be combined to enhance the potential of individual approaches and to complement their weaknesses. So far, large proteins have proven impossible to detect by MS in a single-cell, and it is therefore advisable to combine MS-based methods with other imaging methods such as fluorescence, confocal, or Raman microscopy to independently support compound identification or to “see” other molecules or proteins present in the cell. That information can be effectively used to study the biosynthesis of individual metabolites on the cellular level.

## BIOGRAPHY

Dr. Ales Svatoš is currently independent group leader of the Mass Spectrometry Research Group/Proteomics at Max Planck Institute for Chemical Ecology in Jena (Germany). He obtained his Ph.D. degree in 1986 from the Institute of Chemical Technology (Prague, Czech Republic) and worked at the Institute for Organic Chemistry

and Biochemistry of the Czech Academy of Science until 2001. He spent two years as postdoctoral fellow at Cornell University (1992–1993, Prof. J. Meinwald) and held the Alexander von Humboldt Fellowship at Bonn University (Germany, 1996–1997, Prof. Boland). Since 2002 he has lead the research group in Jena. He is interested in identification of natural products, understanding chemical communications, and developing new MS methods for better understanding of metabolomes and proteomes of the studied organisms. He has authored and co-authored >150 scientific articles and holds several patents. Contact Svatoš at Mass Spectrometry and Proteomics Research Group, Max Planck Institute for Chemical Ecology, Hans-Knoell-Str. 8, 07745 Jena, Germany; Email: svatos@ice.mpg.de.

## ACKNOWLEDGMENT

Financial support from the Max Planck Society is gratefully acknowledged. I thank Emily Wheeler and Bernd Schneider for manuscript editing and Renato Zenobi, Akos Vertes, and Bernhard Spengler for providing articles in press and unpublished materials so as to make the perspective as current as possible. We regret being unable to cite all references on single-cell analysis because of limited space.

## REFERENCES

- (1) Holman, N. Y. N.; Bechtel, H. A.; Hao, Z.; Martin, M. C. *Anal. Chem.* **2010**, *82*, 8757–8765.
- (2) Chan, J.; Fore, S.; Wachsmann-Hogiu, S.; Huser, T. *Laser Photon. Rev.* **2008**, *2*, 325–349.
- (3) Moco, S.; Schneider, B.; Vervoort, J. J. *Prot. Res.* **2009**, *8*, 1694–1703.
- (4) Amantonico, A.; Urban, P. L.; Fagerer, S. R.; Balabin, R. M.; Zenobi, R. *Anal. Chem.* **2010**, *82*, 7394–7400.
- (5) Zare, R. N.; Kim, S. *Ann. Rev. Biom. Eng.* **2010**, *12*, 187–201.
- (6) Wurm, M.; Schopke, B.; Lutz, D.; Muller, J.; Zeng, A. P. *J. Biotech.* **2010**, *149*, 33–51.
- (7) Wang, D. J.; Bodovitz, S. *Trends Biotech.* **2010**, *28*, 281–290.
- (8) Schmid, A.; Kortmann, H.; Dittrich, P. S.; Blank, L. M. *Curr. Op. Biotech.* **2010**, *21*, 12–20.
- (9) Petibois, C. *Anal. Bioanal. Chem.* **2010**, 1–15.
- (10) Amantonico, A.; Urban, P. L.; Zenobi, R. *Anal. Bioanal. Chem.* **2010**, *398*, 2493–2504.
- (11) Petibois, C. *Anal. Bioanal. Chem.* **2010**, *397*, 2051–2065.
- (12) Fernie, A. R.; Trethewey, R. N.; Krotzky, A. J.; Willmitzer, L. *Nature Rev. Mol. Cell Biol.* **2004**, *5*, 763–769.
- (13) Rasche, F.; Svatoš, A.; Maddula, R. K.; Böttcher, C.; Böcker, S. *Anal. Chem.* **2011**, *83*, 1243–1251.
- (14) Fiehn, O.; Kopka, J.; Dormann, P.; Altmann, T.; Trethewey, R. N.; Willmitzer, L. *Nature Biotech.* **2000**, *18*, 1157–1161.
- (15) Schneider, B. *Progr. Bot.* **2011**, *72*, 183–208.
- (16) Saito, K.; Matsuda, F. *Ann. Rev. Plant Biol.* **2010**, *61*, 463–489.
- (17) Jimenez, C. R.; Li, K. W.; Dreisewerd, K.; Spijker, S.; Kingston, R.; Bateman, R. H.; Burlingame, A. L.; Smit, A. B.; van Minnen, J.; Geraerts, W. P. M. *Biochemistry* **1998**, *37*, 2070–2076.
- (18) Caprioli, R. M.; Farmer, T. B.; Gile, J. *Anal. Chem.* **1997**, *69*, 4751–4760.
- (19) Hell, S. W. *Science* **2007**, *316*, 1153–1158.
- (20) Freudiger, C. W.; Min, W.; Saar, B. G.; Lu, S.; Holtom, G. R.; He, C. W.; Tsai, J. C.; Kang, J. X.; Xie, X. S. *Science* **2008**, *322*, 1857–1861.
- (21) Schneider, B.; Holscher, D. *Planta* **2007**, *225*, 763–770.
- (22) Wenzler, M.; Holscher, D.; Oerther, T.; Schneider, B. *J. Exp. Bot.* **2008**, *59*, 3425–3434.
- (23) Lee, S. C.; Kim, K.; Kim, J.; Yi, J. H.; Lee, S.; Cheong, C. *Magn. Res. Imag.* **2009**, *27*, 828–833.



- (24) Slaveykova, V. I.; Guignard, C.; Eybe, T.; Migeon, H. N.; Hoffmann, L. *Anal. Bioanal. Chem.* **2009**, 393, 583–589.
- (25) Musat, N.; Halm, H.; Winterholler, B.; Hoppe, P.; Peduzzi, S.; Hillion, F.; Horreard, F.; Amann, R.; Jorgensen, B. B.; Kuypers, M. M. M. *Proceedings of the Nat. Acad. Sci. U.S.A.* **2008**, 105, 17861–17866.
- (26) Szita, N.; Polizzi, K.; Jaccard, N.; Baganz, F. *Curr. Op. Biotech.* **2010**, 21, 517–523.
- (27) Mellors, J. S.; Jorabchi, K.; Smith, L. M.; Ramsey, J. M. *Anal. Chem.* **2010**, 82, 967–973.
- (28) Shrestha, B.; Vertes, A. *Anal. Chem.* **2009**, 81, 8265–8271.
- (29) Svatos, A. *Trends Biotech.* **2010**, 28, 425–434.
- (30) Dreisewerd, K. *Chem. Rev.* **2003**, 103, 395–425.
- (31) Rottloff, S.; Muller, U.; Kilper, R.; Mithofer, A. *Anal. Biochem.* **2009**, 394, 135–137.
- (32) Tejedor, M. L.; Mizuno, H.; Tsuyama, N.; Harada, T.; Masujima, T. *Anal. Sci.* **2009**, 25, 1053–1055.
- (33) Masujima, T. *Anal. Sci.* **2009**, 25, 953–960.
- (34) Tsuyama, N.; Mizuno, H.; Tokunaga, E.; Masujima, T. *Anal. Sci.* **2008**, 24, 559–561.
- (35) Mizuno, H.; Tsuyama, N.; Date, S.; Harada, T.; Masujima, T. *Anal. Sci.* **2008**, 24, 1525–1527.
- (36) Izumi, Y.; Kajiyama, S.; Nakamura, R.; Ishihara, A.; Okazawa, A.; Fukusaki, E.; Kanematsu, Y.; Kobayashi, A. *Planta* **2009**, 229, 931–943.
- (37) Ebert, B.; Zoller, D.; Erban, A.; Fehrle, I.; Hartmann, J.; Niehl, A.; Kopka, J.; Fisahn, J. *J. Exp. Bot.* **2010**, 61, 1321–1335.
- (38) Lapainis, T.; Rubakhin, S. S.; Sweedler, J. V. *Anal. Chem.* **2009**, 81, 5858–5864.
- (39) Winograd, N.; Garrison, B. J. *Ann. Rev. Phys. Chem.* **2010**, 61, 305–322.
- (40) Fletcher, J. S.; Lockyer, N. P.; Vaidyanathan, S.; Vickerman, J. C. *Anal. Chem.* **2007**, 79, 2199–2206.
- (41) Piehowski, P. D.; Carado, A. J.; Kurczy, M. E.; Ostrowski, S. G.; Heien, M. L.; Winograd, N.; Ewing, A. G. *Anal. Chem.* **2008**, 80, 8662–8667.
- (42) Carado, A.; Kozole, J.; Passarelli, M.; Winograd, N.; Loboda, A.; Wingate, J. *Appl. Surf. Sci.* **2008**, 255, 1610–1613.
- (43) Holscher, D.; Shroff, R.; Knop, K.; Gottschaldt, M.; Crecelius, A.; Schneider, B.; Heckel, D. G.; Schubert, U. S.; Svatos, A. *Plant J.* **2009**, 60, 907–918.
- (44) Rompp, A.; Guenther, S.; Schober, Y.; Schulz, O.; Takats, Z.; Kummer, W.; Spengler, B. *Angew. Chem., Int. Ed.* **2010**, 49, 3834–3838.
- (45) Guenther, S.; Rompp, A.; Kummer, W.; Spengler, B. *Intern. J. Mass Spectrom.* doi: 10.1016/j.ijms.2010.11.011.
- (46) Bouschen, W.; Schulz, O.; Eikely, D.; Spengler, B. *Rapid Commun. Mass Spectrom.* **2010**, 24, 355–364.
- (47) Amantonico, A.; Urban, P. L.; Oh, J. Y.; Zenobi, R. *Chimia* **2009**, 63, 185–188.
- (48) Amantonico, A.; Oh, J. Y.; Sobek, J.; Heinemann, M.; Zenobi, R. *Angew. Chem., Int. Ed.* **2008**, 47, 5382–5385.
- (49) Urban, P. L.; Amantonico, A.; Fagerer, S. R.; Gehrig, P.; Zenobi, R. *Chem. Commun.* **2010**, 46, 2212–2214.
- (50) Stadler, J.; Schmid, T.; Zenobi, R. *Nano Lett.* **2010**, 10, 4514–4520.
- (51) Urban, P. L.; Jefimovs, K.; Amantonico, A.; Fagerer, S. R.; Schmid, T.; Madler, S.; Puigmarti-Luis, J.; Goedecke, N.; Zenobi, R. *Lab on Chip* **2010**, 10, 3206–3209.
- (52) Amantonico, A.; Flamigni, L.; Glaus, R.; Zenobi, R. *Metabolomics* **2009**, 5, 346–353.
- (53) Miura, D.; Fujimura, Y.; Yamato, M.; Hyodo, F.; Utsumi, H.; Tachibana, H.; Wariishi, H. *Anal. Chem.* **2010**, 82, 9789–9796.
- (54) Urban, P. L.; Schmid, T.; Amantonico, A.; Zenobi, R. *Anal. Chem.* **2011**, 83, 1843–1849.
- (55) Zimmerman, T. A.; Rubakhin, S. S.; Romanova, E. V.; Tucker, K. R.; Sweedler, J. V. *Anal. Chem.* **2009**, 81, 9402–9409.
- (56) Shrestha, B.; Nemes, P.; Vertes, A. *Appl. Phys. A: Mater. Sci. Process.* **2010**, 101, 121–126.
- (57) Nemes, P.; Barton, A. A.; Li, Y.; Vertes, A. *Anal. Chem.* **2008**, 80, 4575–4582.
- (58) Nemes, P.; Barton, A. A.; Vertes, A. *Anal. Chem.* **2009**, 81, 6668–6675.
- (59) Shrestha, B.; Patt, J. M.; Vertes, A. *Anal. Chem.* **2011**, 83, 2947–2955.
- (60) Bradshaw, J. A.; Ovchinnikova, O. S.; Meyer, K. A.; Goeringer, D. E. *Rapid Commun. Mass Spectrom.* **2009**, 23, 3781–3786.
- (61) Schmitz, T. A.; Gamez, G.; Setz, P. D.; Zhu, L.; Zenobi, R. *Anal. Chem.* **2008**, 80, 6537–6544.